

SOLUTION OF THE PROBLEM OF INTERACTION OF RAYLEIGH WAVES WITH THE EDGE OF A WEDGE WITH A SMALL APEX ANGLE

Kh. B. Tolipov

UDC 539.25

The problem of interaction of Rayleigh waves with the edge of a wedge with a small apex angle was solved using classical methods. This solution describes surface waves whose characteristics agree with well-known experimental data and bulk waves which have a significant effect on energy distribution. New features of surface wave propagation in wedge-shaped bodies are revealed.

Key words: *inhomogeneous wave, diffraction, wedge-shaped medium, wave field, elasticity theory.*

Introduction. Difficulties in the solution of the problem of interaction of Rayleigh waves with the edge of a wedge with a small apex angle are due to the complexity of the acoustic processes occurring near the edge of the wedge. The present work is a continuation of studies [1–3], which showed that in a Rayleigh wave, the directions of the wave normal of shear and longitudinal components do not coincide with the direction of wave propagation. This indicates acoustic anisotropy on the interface between the media and leads to unusual phenomena observed during reflection of the wave from the wedge faces.

The wave field in a wedge is a set of four waves: the incident surface wave, the wave reflected from the edge of the wedge, the wave propagating to the second face of the wedge, and transformed bulk waves. The structure of Rayleigh waves is characterized by the presence of displacements localized near the surface. In approaching the edge, the displacements reach the opposite face of the wedge and cause perturbations of the this face, resulting in secondary waves. Because these perturbations are inhomogeneous, both surface and bulk waves arise which transfer energy in a direction opposite to the edge of the wedge. Therefore, in the case $\theta < 90^\circ$, the parameters and spatial structure of the acoustic field incident on the edge change when the displacements reach the second face of the wedge.

The evolution of the structure of the incident Rayleigh wave during motion from infinity to the edge of the wedge was investigated in [3], where an approximate solution of the wave problem considered was obtained using classical methods. To satisfy the condition of the absence of stresses on the faces of the wedge, the wave vector k should take complex values whose real part defines the wave velocity and whose imaginary part defines the decay due to energy outflow during transformation into bulk waves.

Calculations show that, in approaching the edge, the wave is divided into two modes — antisymmetric and symmetric, whose spectral characteristics become similar to the characteristics of bulk waves (Fig. 1). As the wedge angle decreases, changes in the phase velocity are manifested in a certain increase in the steepness of the wave with increasing local thickness of the wedge at the location of this wave.

We note that in elastic media, the propagation velocity of an ultrasonic wave remains constant, whereas in a wedge-shaped plate, it varies monotonically when approaching the edge of the wedge: the velocity of the symmetric mode increases and tends to the longitudinal wave velocity, and the velocity of the antisymmetric mode decreases to zero.

South-Ural State University, Chelyabinsk 454080; thb@susu.ac.ru. Translated from *Prikladnaya Mekhanika i Tekhnicheskaya Fizika*, Vol. 51, No. 1, pp. 29–38, January–February, 2010. Original article submitted March 11, 2009.

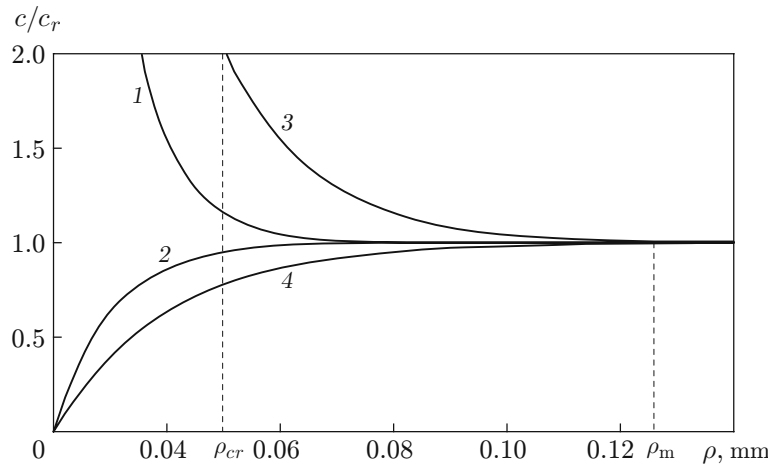


Fig. 1. Rayleigh wave velocity versus distance to the breakpoint for $\theta = 20^\circ$ (1 and 2) and 10° (3 and 4); curves 1 and 3 refer to the symmetric mode and curves 2 and 4 to the antisymmetric mode.

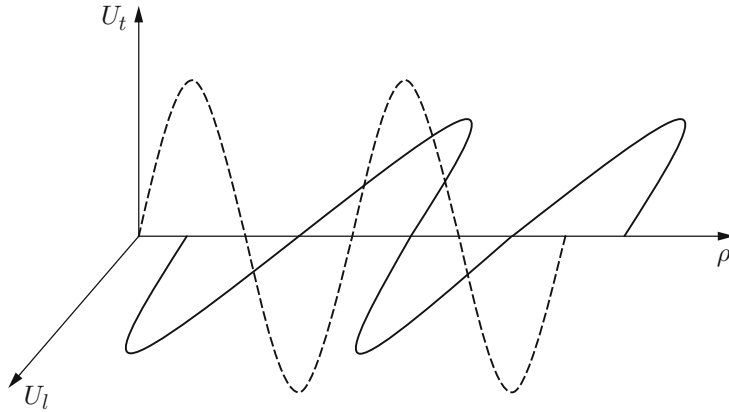


Fig. 2. Displacement in Rayleigh wave: solid curves refer to longitudinal waves, and dashed curves to shear waves.

The nature of wave propagation in a wedge-shaped plate differs from that in a plane-parallel plate in that the waves in which the particle displacements are antisymmetric about the plane of symmetry of the wedge reach its edge. Symmetric waves reach only a certain critical point ρ_{cr} , without reaching the edge of the wedge. The sizes of the region (plug) into which longitudinal oscillations do not penetrate depend greatly on the size of the wedge angle. The upper boundary of this region ρ_m is found from the condition of multiplicity of the roots of the dispersion equation. At this point, the branches of the antisymmetric and symmetric modes merge.

The change in the displacement amplitudes of the wave reflected from the wedge angle is due to interference factors. As the wedge angle changes, superposition of the phases of the antisymmetric and symmetric components is responsible for oscillations reflection coefficients for small wedge angles.

At the point of merging of the branches of the antisymmetric and symmetric modes ρ_m , the reflection from the edge gives rise to a Rayleigh wave which is a set of longitudinal and transverse components [4]:

$$\mathbf{U}_r = \mathbf{U}_t + \mathbf{U}_l.$$

It is necessary to note that the components of the Rayleigh wave are related to each other and are shifted in phase by 90° (Fig. 2). The longitudinal component propagates along the surface, and the transverse component propagates along the normal to it. During motion, there is a gradual energy redistribution from one component to the other; therefore, they are two integral components of the Rayleigh waves just as electric and magnetic fields are the components of a unified electromagnetic field.

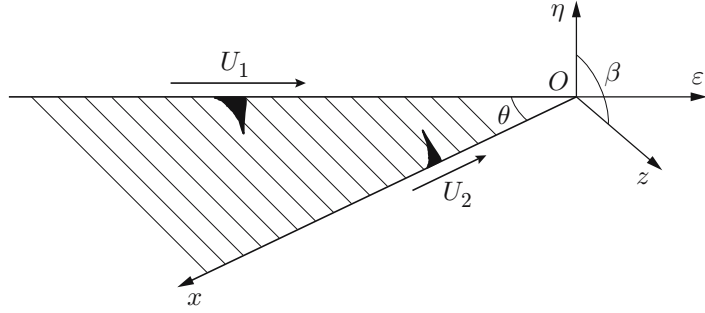


Fig. 3. Diagram of interaction of a Rayleigh waves with a wedge.

1. Formulation of the Problem. We consider a theoretical model for the propagation of an acoustic wave from infinity to the edge of the wedge. An incident harmonic surface Rayleigh wave U_1 , propagating on the upper face of the wedge to the breakpoint O , causes an inhomogeneous perturbation of the part of the surface on the lower face (Fig. 3).

The dynamic model of Rayleigh wave propagation in a wedge-shaped medium is constructed on the basis of the equation of motion and boundary conditions assuming zero stresses on the surfaces of the wedge.

The wave field of the initial wave is written in the coordinate system (ε, η) , and the wave field behind the break is studied using a coordinate system (x, z) that can be obtained by rotation of the initial coordinate system by angle β . It is required to determine the displacement and velocity fields in the region behind the surface break at various times.

The displacements U_l and U_t in the longitudinal and transverse waves can be determined from the standard equations of acoustics for an isotropic solid:

$$\Delta \mathbf{U}_l + k_l^2 \mathbf{U}_l = 0, \quad \Delta \mathbf{U}_t + k_t^2 \mathbf{U}_t = 0 \quad (1)$$

with the following boundary conditions at $z = 0$:

$$\mu \left(\frac{\partial \mathbf{U}_z}{\partial x} + \frac{\partial \mathbf{U}_x}{\partial z} \right) + \sigma_{xz}^0 = 0, \quad 2\mu \frac{\partial \mathbf{U}_z}{\partial z} + \lambda \left(\frac{\partial \mathbf{U}_z}{\partial x} + \frac{\partial \mathbf{U}_x}{\partial z} \right) + \sigma_{zz}^0 = 0. \quad (2)$$

Here $k_l = \omega/c_l$, $k_t = \omega/c_t$ and c_l , c_t are the wavenumbers and propagation velocities of longitudinal and transverse waves, respectively, ω is the circular frequency, σ_{xz}^0 , σ_{zz}^0 are the stresses caused by displacements of the initial Rayleigh wave on the surface behind the break, λ and μ are Lamé constants, and \mathbf{U}_z and \mathbf{U}_x are the projections of the displacements u_z and u_x onto the z and x axes.

Introducing the longitudinal and transverse potentials linked to the displacements by the relations $\mathbf{U}_l = \text{grad } \Phi$ and $\mathbf{U}_t = \text{rot } \Psi$, we write system (1), (2) in the form

$$\Delta \Phi + k_l^2 \Phi = 0, \quad \Delta \Psi + k_t^2 \Psi = 0; \quad (3)$$

$$\mu \left(2 \frac{\partial^2 \Phi}{\partial x \partial z} + \frac{\partial^2 \Psi}{\partial x^2} + \frac{\partial^2 \Psi}{\partial z^2} \right) = -\sigma_{xz}^0, \quad 2\mu \left(-\frac{\partial^2 \Phi}{\partial x^2} - \frac{k_t^2}{2} \Phi + \frac{\partial^2 \Psi}{\partial z \partial x} \right) = -\sigma_{zz}^0. \quad (4)$$

Oscillations on the inclined plane are generated by an incident plane Rayleigh wave whose spatial structure is described by the formulas

$$\Phi_r = \exp(i k_r \varepsilon - i \omega t + q_r \eta), \quad \Psi_r = p \exp(i k_r \varepsilon - i \omega t + s_r \eta), \quad (5)$$

where

$$q_r = \sqrt{k_r^2 - k_l^2}, \quad s_r = \sqrt{k_r^2 - k_t^2}, \quad p = -i \sqrt{q_r/s_r}.$$

(Below, the dependence on time is omitted.)

Using relations (5) and the standard methods of acoustics for the stress tensor in the initial Rayleigh wave, we obtain

$$\sigma_{\varepsilon \eta} = [P(k_r) \exp(q\eta) + Q(k_r) \exp(s\eta)] \exp(i k_r \varepsilon), \quad \sigma_{\eta \eta} = [R(k_r) \exp(q\eta) + S(k_r) \exp(s\eta)] \exp(i k_r \varepsilon),$$

where $P(k_r) = 2k_r q_r$, $Q(k_r) = k_r^2 + s_r^2$, $S(k_r) = -2k_r s_r$, and $R(k_r) = 2k_r^2 - k_t^2$. Using the formulas of transformation from the coordinate system (ε, η) to the system (x, z)

$$x = \eta \cos \beta - \varepsilon \sin \beta, \quad z = \eta \sin \beta + \varepsilon \cos \beta,$$

we write the expressions for the stress tensor component in the initial Rayleigh wave in the coordinates (x, z) in the following form [5]:

$$\sigma_{xz}^0 = \sigma_{xz}^x \sin \beta + \sigma_{zz}^z \cos \beta, \quad \sigma_{zz}^0 = \sigma_{xz}^z \sin \beta + \sigma_{zz}^x \cos \beta, \quad (6)$$

where

$$\sigma_{xz}^x = P(k_{1x}) \exp(ik_{1x}x) + pQ(k_{2x}) \exp(ik_{2x}x),$$

$$\sigma_{zz}^x = R(k_{1x}) \exp(ik_{1x}x) + pS(k_{2x}) \exp(ik_{2x}x),$$

$$\sigma_{xz}^z = P(k_{1z}) \exp(ik_{1z}x) + pQ(k_{2z}) \exp(ik_{2z}x),$$

$$\sigma_{zz}^z = R(k_{1z}) \exp(ik_{1z}x) + pS(k_{2z}) \exp(ik_{2z}x).$$

In expressions (6), the projections of the longitudinal and shear components of the wave vector of the initial Rayleigh waves onto the coordinate axis x and z are represented in complex form

$$k_{1x} = k_r \cos \beta + iq_r \sin \beta, \quad k_{1z} = k_r \cos \beta + is_r \sin \beta,$$

$$k_{2x} = k_r \sin \beta + iq_r \cos \beta, \quad k_{2z} = k_r \sin \beta + is_r \cos \beta.$$

2. Construction of the Solution. The solution of the wave equations for potentials (3) can be written as the spectral decomposition

$$\Phi = \frac{1}{2\pi} \int_{-\infty}^{\infty} \Phi^*(k) e^{-ikx} dk, \quad \Psi = \frac{1}{2\pi} \int_{-\infty}^{\infty} \Psi^*(k) e^{-ikx} dk.$$

In this problem, the expressions for the wave perturbations on the lower face of the wedge

$$\sigma_{xz}^* = \frac{1}{2\pi} \int_{-\infty}^{\infty} \sigma_{xz}^0 e^{ikx} dx = \frac{1}{2\pi} \left(\frac{P(k_{1x})}{k - k_{1x}} + p \frac{Q(k_{2x})}{k - k_{2x}} \right) \cos \beta + \frac{1}{2\pi} \left(\frac{R(k_{1z})}{k - k_{1z}} + p \frac{S(k_{2z})}{k - k_{2z}} \right) \sin \beta,$$

$$\sigma_{zz}^* = \frac{1}{2\pi} \int_{-\infty}^{\infty} \sigma_{zz}^0 e^{ikx} dx = \frac{1}{2\pi} \left(\frac{R(k_{1x})}{k - k_{1x}} + p \frac{S(k_{2x})}{k - k_{2x}} \right) \cos \beta + \frac{1}{2\pi} \left(\frac{P(k_{1z})}{k - k_{1z}} + p \frac{Q(k_{2z})}{k - k_{2z}} \right) \sin \beta$$

take the form of spatial harmonics. From solutions (3) and boundary conditions (4), we obtain the system of homogeneous algebraic equations for the wave potentials.

Using the inverse Fourier transform, we obtain the relations between the complex amplitudes of the potentials and the wedge angle:

$$\begin{aligned} \Phi &= \frac{1}{2\pi} \int_{-\infty}^{\infty} \frac{1}{4k^2 qs - (k^2 + s^2)^2} \left\{ \left[\left(\frac{P(k_{1x})}{k - k_{1x}} - p \frac{Q(k_{1x})}{k - k_{2x}} \right) S(k_r) + \left(\frac{R(k_{1x})}{k - k_{1x}} - p \frac{S(k_{2x})}{k - k_{2x}} \right) Q(k_r) \right] \cos \beta \right. \\ &\quad \left. + \left[\left(\frac{P(k_{1z})}{k - k_{1z}} - p \frac{Q(k_{2z})}{k - k_{2z}} \right) S(k_r) + \left(\frac{R(k_{1z})}{k - k_{1z}} - p \frac{S(k_{2z})}{k - k_{2z}} \right) Q(k_r) \right] \sin \beta \right\} \exp(qz) dk, \\ \Psi &= \frac{1}{2\pi} \int_{-\infty}^{\infty} \frac{1}{4k^2 qs - (k^2 + s^2)^2} \left\{ \left[\left(\frac{P(k_{1x})}{k - k_{1x}} - p \frac{Q(k_{1x})}{k - k_{2x}} \right) R(k_r) + \left(\frac{R(k_{1x})}{k - k_{1x}} - p \frac{S(k_{2x})}{k - k_{2x}} \right) P(k_r) \right] \cos \beta \right. \\ &\quad \left. + \left[\left(\frac{P(k_{1z})}{k - k_{1z}} - p \frac{Q(k_{2z})}{k - k_{2z}} \right) R(k_r) + \left(\frac{R(k_{1z})}{k - k_{1z}} - p \frac{S(k_{2z})}{k - k_{2z}} \right) P(k_r) \right] \sin \beta \right\} \exp(sz) dk. \end{aligned} \quad (7)$$

Representation (7) gives the exact wave pattern in space for both bulk and surface waves.

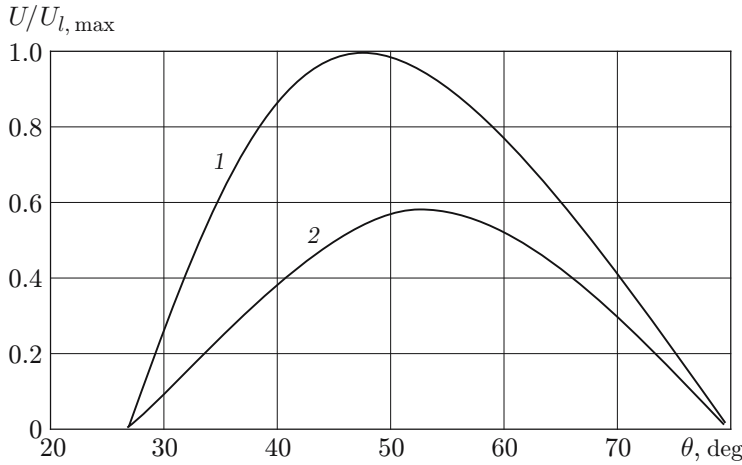


Fig. 4. Displacement amplitudes (normalized to the maximum displacement of the longitudinal wave) in bulk waves versus wedge angle: 1) longitudinal waves; 2) shear waves.

Using the saddle-point method to transform to the integral representation of solution (7), we obtain

$$\begin{aligned}
U_l &= \sqrt{\frac{2\pi}{k_l\rho}} \frac{\cos^2\gamma}{k_l^3 D_l} \left[\left(p \frac{2k_{2x}^2 - k_t^2}{k_l \sin\gamma - k_{2x}} - \frac{2k_{1x}\sqrt{k_l^2 - k_{1x}^2}}{k_l \sin\gamma - k_{1x}} \right) 2k\sqrt{k^2 - k_t^2} \right. \\
&\quad \left. + \left(p \frac{2k_{2x}\sqrt{k_t^2 - k_{2x}^2}}{k_l \sin\gamma - k_{2x}} + \frac{2k_{1x}^2 - k_t^2}{k_l \sin\gamma - k_{1x}} \right) (2k_r^2 - k_t^2) \right] \exp\left(ik_l\rho - i\frac{\pi}{4}\right), \\
U_t &= \sqrt{\frac{2\pi}{k_t\rho}} \frac{\cos^2\gamma}{k_t^3 D_t} \left[\left(p \frac{2k_{2x}^2 - k_t^2}{k_t \sin\gamma - k_{2x}} - \frac{2k_{1x}\sqrt{k_l^2 - k_{1x}^2}}{k_t \sin\gamma - k_{1x}} \right) 2k\sqrt{k^2 - k_t^2} \right. \\
&\quad \left. + \left(p \frac{2k_{2x}\sqrt{k_t^2 - k_{2x}^2} - k_{2x}^2}{k_t \sin\gamma - k_{2x}} + \frac{2k_{1x}^2 - k_t^2}{k_t \sin\gamma - k_{1x}} \right) (2k_r^2 - k_t^2) \right] \exp\left(ik_t\rho - i\frac{\pi}{4}\right),
\end{aligned} \tag{8}$$

where γ is the azimuthal angle reckoned from the z axis, $D_l = 4\sin^2\gamma\cos^2\gamma\sqrt{\sin^2\gamma - \varepsilon^2} - (2\sin^2\gamma - 1)^2$, $\varepsilon = k_t/k_l$, and $D_t = 4\sin^2\gamma\cos^2\gamma\sqrt{\sin^2\gamma - \varepsilon^2} - (2\sin^2\gamma - \varepsilon^2)^2$.

We note that relations (8) describe the displacement amplitudes in the bulk waves arising on the lower face of the wedge upon single reflection.

An analysis of solution (7) shows that the amplitude of the bulk waves is determined by the longitudinal and shear components of the incident wave and depends on the structure of the wave perturbation profile on the lower face of the wedge. This is supported by the nonmonotonic nature of the transformation of the surface waves to bulk waves (Fig. 4) which arise when the projection of the wave vector of the Rayleigh wave onto the surface of the opposite face of the wedge is smaller than the projection of the shear wave vector:

$$\theta_0 \geq \arccos(k_t/k_r).$$

It is necessary to note that the results of the study performed coincide with the results of the solution obtained in [1]. Indeed, in the formulation of the problem, only the projections of the vectors change, but for both large and small wedge angles, the projections of the vectors take the same values. In particular, at large angles ($90^\circ \leq \theta \leq 180^\circ$), the projection of the vector $k_{1x}(\theta) = k_r \cos\beta + iq_r \sin\beta$ onto the x axis for the real part of the expression varies from the maximum to minimum values, and in the solution obtained for small angles θ ($0^\circ \leq \theta \leq 90^\circ$), this projection takes the same values but in the reverse direction.

The residues at the poles of the subintegral expression (7) determine the parameters of the surface Rayleigh waves propagating along the boundary.

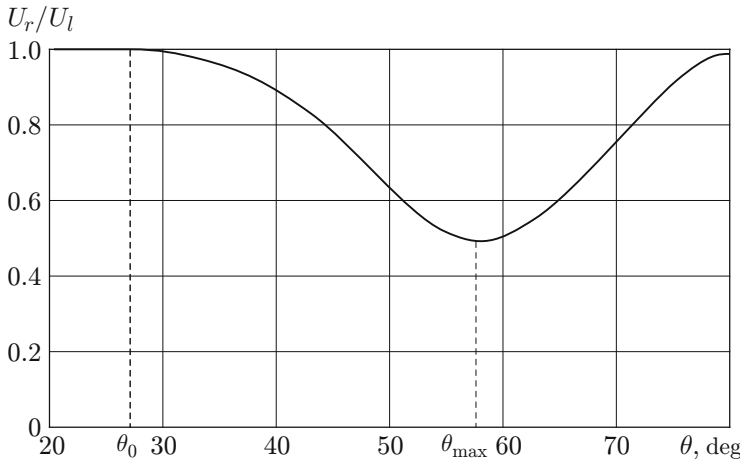


Fig. 5. Normalized displacement amplitudes in the Rayleigh wave on the lower face versus wedge angle.

Figure 5 shows the normalized displacement amplitude in the Rayleigh wave on the lower face versus wedge angle for an aluminum sample calculated by the formula

$$U_x = \frac{\partial \Phi}{\partial x} - \frac{\partial \Psi}{\partial z}. \quad (9)$$

An analysis of the results shows that, at small wedge angles ($\theta < \theta_0$), the displacement amplitude in the wave first remains constant and then varies due to the influence of the normal and shear components of the wave perturbations caused by the incident wave. At small wedge angles, the dissipated acoustic field is significantly affected by the tangential components of the perturbing forces; as the wedge angle increases, the effect of the normal component of these forces becomes a determining factor. At a wedge angle θ_{\max} , the displacement amplitude of the Rayleigh waves takes the minimum value, indicating the maximum transformation of the surface wave to a bulk wave. It should be noted that, for $\theta < \theta_0$, the projection of the wave vector k of the wave incident onto the edge onto the lower face of the wedge is larger than the projections of the vectors of the shear k_t and longitudinal k_l waves but smaller than the projections of the vectors of the Rayleigh wave: $k_l < k_t < k \leq k_r$. In this case, the velocity of wave perturbations on the surface are smaller than the phase velocities of shear and longitudinal waves in the medium but larger than the velocity of the surface Rayleigh wave. The generated inhomogeneous waves are unstable, and their spatial structure varies with time.

The decrease in the velocities of the generated inhomogeneous waves to the Rayleigh wave velocity is due to two factors. First, at the interface in solids, longitudinal and shear waves transform into each other. As a result, the propagation velocity of the surface wave consisting of shear and longitudinal components decreases gradually since the shear wave moves more slowly than the longitudinal wave. Second, as the wave velocity decreases, the thickness of the boundary wave layer increases and its spatial structure changes. As a result, the wave energy density decreases, spreading over a larger volume. The velocity of the surface wave also decreases monotonically until the velocities of the longitudinal and shear components become equal to the Rayleigh wave velocity. This effect is observed in solids and has no analog in other media.

It should be noted that the wave normal direction of the longitudinal component, which is defined by the formula

$$\alpha_0 = \arccos(k_l/k_r),$$

coincides with the direction of the normal to the wedge face at an angle equal to the wedge angle θ . Hence, at this angle, the perturbations on the lower face take maximum values, resulting in the arrival of the incident Rayleigh waves at this face.

Thus, it is possible to distinguish two characteristic regions. For angles $0 < \theta < \theta_0$, the spatial structure of the Rayleigh wave induced on the lower face of the wedge, remains constant. For $\theta > \theta_0$, wave splits into surface and bulk components, the latter having a significant effect on the energy distribution.

The obtained result is approximate. In the approach described above, the parameters of the incident Rayleigh wave ahead of the edge are assumed to be constant, which is valid only for large wedge angles [1]. In this case, the energy of the wave is expended in the generation of secondary waves. In the case considered, approaching the edge, the incident Rayleigh wave interacts with the opposite face and its structure changes due to energy outflow during transformation of bulk waves. The Rayleigh wave generated on any face of the wedge causes secondary (bulk and Rayleigh) waves on the opposite face. In this case, because of spatial symmetry, the shape of the wave perturbation profile does not change. This processes continues until the wave perturbation amplitude become equal to zero because, upon at each reflection, the induced bulk waves carry away energy. Thus, a Rayleigh wave moves over each face toward the edge of the wedge, and the parameters of these waves depend on the size of the wedge angle and the location of the wave. Because of spatial symmetry, it can be assumed that, on these faces of the wedge, the energy of the incident wave is equally distributed between the waves. Consequently, the structure and parameters of the surface and bulk waves on the lower and upper faces of the wedge are identical, and the displacement amplitudes in the waves are equal to half of the amplitude obtained in (9).

The induced Rayleigh wave on the lower face is reflected when colliding with the edge of the wedge. The symmetric mode of this wave is reflected at a critical distance from the edge and, summing with the antisymmetric mode reflected from the edge, determines the acoustic field on this face of the wedge.

Because upon reflection, the antisymmetric and symmetric modes of the Rayleigh wave near the edge travel different distances (see Fig. 1), for the merging of these modes at the point ρ_m , the amplitude of the Rayleigh waves is determined by the superposition of their phases:

$$U_r = \sqrt{U_s^2 + U_a^2 + 2U_s U_a \cos(\delta\varphi)}. \quad (10)$$

As the wedge angle varies, the displacement amplitude in relation (10) vary. The induced Rayleigh wave retains structure up to the point ρ_m , but its amplitude decreases due to the occurrence of bulk waves (see Fig. 5). For the same reason, the transformation to the bimodal structure at a constant wedge angle also occurs with a decrease in the amplitude. However, because the modes travels different distances and have different damping coefficients, the amplitude of displacements in the antisymmetric mode at the point of Rayleigh wave formation is lower than that in the symmetric mode. This leads to a change in the maximum and minimum values of the oscillation amplitudes in the Rayleigh wave upon reflection from the edge of the wedge.

For convenience of the further calculations, we approximate the theoretically obtained curves of the velocities of the symmetric mode $V_s(\rho)$ and antisymmetric mode $V_a(\rho)$ by the relations

$$V_a(\rho) = 1 - \exp(-2\rho), \quad V_s(\rho) = \exp(\rho - 0.76)^{-2.5}.$$

Then, in view of the direct and reverse directions of motion, the superposition of the phases of the interfering waves is defined as

$$\delta\varphi = \frac{2\pi}{T} \left(2 \int \frac{d\rho}{V_a(\rho)} + 2 \int \frac{d\rho}{V_s(\rho)} \right).$$

For the antisymmetric mode, the integration over ρ is performed from zero to the critical distance ρ_m , and for the symmetric mode, it is performed from the characteristic distance ρ_{cr} to ρ_m (see Fig. 1).

Figure 6a shows the dependence of the normalized displacement amplitudes in the reflected Rayleigh wave on the lower face of the wedge. It is evident that a decrease in the wedge angle leads to a reduction in the period oscillations because of the faster change in the phase difference between two modes upon their reflection. The oscillation amplitude, in contrast, increases, which is due, as noted above, to the attenuation of bulk waves at small wedge angles.

The incident Rayleigh wave on the upper face of the wedge is also reflected when interacting with the edge of the wedge. The symmetric mode of this wave is reflected at a critical distance from the edge and, combining with the antisymmetric mode reflected from the edge, determines the acoustic field on this face of the wedge. We note that, at the point of Rayleigh wave formation, oscillations occur in antiphase. Hence, the reflected Rayleigh wave generated on the upper face of the wedge can be represented as the result of superposition of oscillations:

$$U_{rp} = \sqrt{U_l^2 + U_t^2 - 2U_l U_t \cos(\delta\varphi)}$$

and the acoustic field on this face of the wedge can be determined using the procedure proposed here.

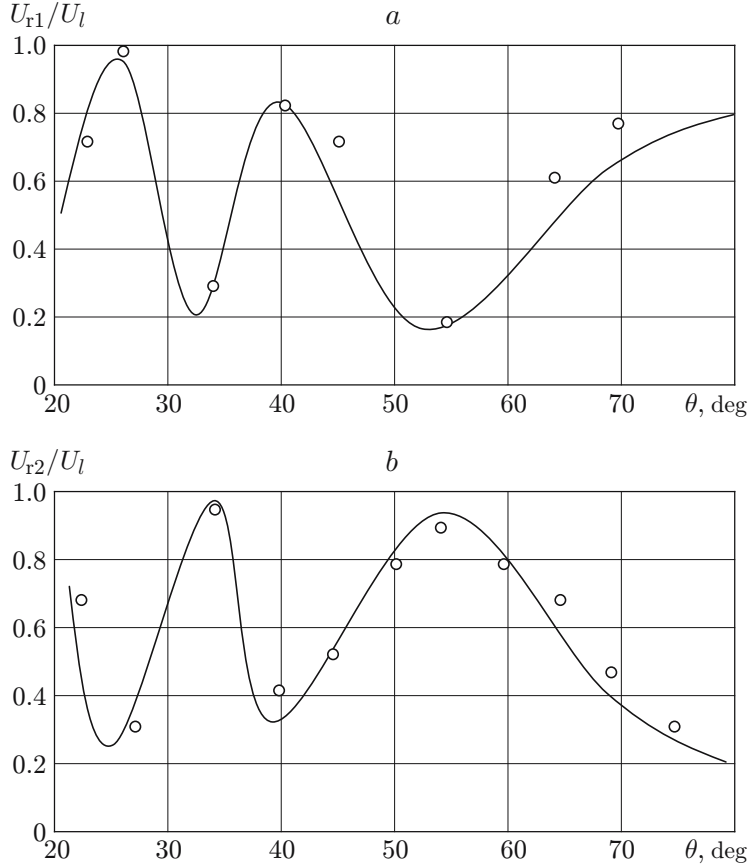


Fig. 6. Normalized displacement amplitude in the reflected Rayleigh wave on the lower (a) and upper (b) faces of the wedge versus wedge angle: curves refer to calculations, and points to experimental data [4].

It is necessary to note that the maxima of the displacement amplitudes in the waves on the upper face of the wedge (Fig. 6b) correspond to the minima on the lower face (see Fig. 6a), and vice versa. Because energy fluxes are coupled with wave propagation, to satisfy the energy conservation law, it is necessary to keep balance between the fluxes associated with both surface and volume waves on the upper and lower faces. Hence, a decrease in the displacement amplitude of Rayleigh waves on one face leads to its increase on the other face, and a decrease in the maximum displacement amplitude with decreasing wedge angle indicates attenuation of the generated bulk waves.

Conclusions. The problem of diffraction of Rayleigh waves incident on an inclined plane at a small angle was solved. From the analysis of the solutions obtained, it follows that the proposed theoretical model describing the variation in the oscillation amplitudes of reflected Rayleigh wave at small wedge angles agrees with the experimentally observed wave dynamics. The physical aspects of the occurrence of the reflected field of the surface waves caused by the incidence of an inhomogeneous wave on an inclined plane were analyzed. It was found that the transformation of the Rayleigh waves to a bulk wave is the main mechanism determining the oscillation energy loss upon the arrival of the surface wave to the inclined plane.

The investigation of the diffraction of surface waves at small wedge angles revealed a number of interesting effects and provides a better understanding of the properties of inhomogeneous Rayleigh waves.

REFERENCES

1. S. Yu. Gurevich and Kh. B. Tolipov, “Diffraction of surface waves by the edge of a wedge,” *J. Appl. Mech. Tech. Phys.*, **44**, No. 5, 736–740 (2003).
2. V. D. Buchel’nikov, S. Yu. Gurevich, H. B. Tolipov, “Diffraction of an inhomogeneous wave by an inclined surface,” in: *18th Sessions of Ross. Akust. Ob-va*, Vol. 1, Geos, Moscow (2006), pp. 171–173.
3. Kh. B. Tolipov “Two-dimensional problem of propagation of acoustic oscillations in a wedge,” *Mat. Model.*, **15**, No. 10, 105–108 (2003).
4. I. A. Viktorov, *Physical Fundamentals of Engineering Applications of Ultrasonic Rayleigh and Lamb Waves* [in Russian], Nauka, Moscow (1966).
5. Yu. N. Rabotnov, *Mechanics of a Deformable Solid* [in Russian], Nauka, Moscow (1988).